ELSEVIER

Spectrochimica Acta Part B 56 (2001) 2465–2478

SPECTROCHIMICA ACTA PART B

www.elsevier.com/locate/sab

Estimation of the emission temperature of an electrodeless discharge lamp and determination of the oscillator strength for the I($^2P_{3/2}$) 183.038 nm resonance transition

Peter Spietz[a,*], Uldis Gross[b], Edgars Smalins[b], Johannes Orphal[c], John P. Burrows[a]

[a] *Institute of Environmental Physics (IUP), University of Bremen, P.O. Box 330440, 28334 Bremen, Germany*
[b] *Institute of Atomic Physics and Spectroscopy, University of Latvia, Raina Blvd. 19, Riga, LV-1586, Latvia*
[c] *Laboratoire de Photophysique Moléculaire, CNRS, Bât. 350, Université de Paris-Sud, 91405 Orsay Cedex, France*

Received 16 May 2001; accepted 23 August 2001

Abstract

The 183.038 nm resonance absorption transition of I($^2P_{3/2}$) has been studied using a flash photolysis set-up for gas-phase chemistry and a radio frequency powered electrodeless discharge lamp filled with iodine. The dependence of self-absorption and self-reversal on iodine partial pressure in the discharge volume was measured. The optimum iodine partial pressure, with self-absorption minimized and acceptable intensity, is determined to be approximately 2.5×10^{-3} mbar. A method is described to estimate the temperature of the emitting atoms using direct measurements of relative absorption at different absorber concentrations. This yields an emission temperature of 923 ± 50 K. Using this temperature, the oscillator strength for the I($^2P_{3/2}$) transition at 183.038 nm is determined to be $f = (3.87 \pm 0.57) \times 10^{-3}$, corresponding to an absorption cross-section at the center of the line of $\sigma = (5.42 \pm 0.8) \times 10^{-14}$ cm^2 atom^{-1} This shows a difference from one of two earlier measurements, but is close to the other. The remaining difference from the latter measurement is probably due to tendencies of opposite biases inherent to the experiments.

Keywords: Iodine; I($^2P_{3/2}$); Electrodeless discharge lamp; Emission temperature determination; Oscillator strength; Absorption cross-section

* Corresponding author. Fax: +49-421-218-4555.
E-mail address: peter.spietz@iup.physik.uni-bremen.de (P. Spietz).

0584-8547/01/$ - see front matter
PII: S0584-8547(01)00330-5

1. Introduction

Laboratory studies of the gas phase chemistry of iodine and ozone, performed to improve our understanding of the chemistry of iodine oxides in the Earth's atmosphere, have recently been published (see [1–6], and references therein). However, none of these studies experimentally observed the formation and decay of $I(^2P_{3/2})$ and $I(^2P_{1/2})$ to estimate their contribution to the temporal behavior of IO or OIO. Earlier studies performed in this laboratory [5] clearly indicated the significance of an accurate knowledge of the varying content of free iodine atoms in studies of chemical kinetics and quantitative spectroscopy of iodine monoxide, IO, and iodine dioxide, OIO, radicals.

Electrodeless discharge lamps (EDL) are well known as intense sources of a variety of atomic emissions in the ultraviolet spectral region [7,8]. Recently, the development and first study of an inexpensive and convenient EDL iodine line source, powered by radio frequency (RF), were reported [8]. In the present study a flash photolysis set-up designed for the investigation of gas phase chemistry of iodine oxides was combined with a resonance absorption set-up using the newly developed iodine EDL. The operating conditions of the EDL have been optimized and the relevant oscillator strength has been determined for the purpose of later using an EDL for quantitative spectroscopy of iodine atoms and their reactions.

A crucial factor in the determination of the emission line profile of the EDL is the temperature of the emitting discharge volume, yet in general, this quantity is not directly accessible. An indirect method has been developed using the mathematical concept of relative absorption of emission and absorption lines of different line widths. These lines are assumed to have Doppler line shape. The source temperature can be inferred from different relative absorptions measured with an EDL at various absorber concentrations. This knowledge is then used to estimate the oscillator strength for the atomic transition [$I(^2P_{3/2})$ at 183.038 nm].

2. Experimental

A schematic diagram of the apparatus is shown in Fig. 1. It comprises a reaction vessel, flash photolysis system, UV-visible grating spectrometer and a charge-coupled device (CCD) camera as detection system. The reaction vessel consists of a double-jacketed quartz tube and is temperature-stabilized by a flow of ethanol from a thermostatic bath. The optical windows at the front and back end of the vessel are made from fused silica and are double-walled and evacuated for thermal insulation. A 250-W tungsten lamp was used for absorption spectroscopy of I_2 between 350 and 650 nm. After having traversed the vessel twice (flip mirror 1 in place and flip mirror 2 flipped aside, see Fig. 1), the analysis light was focussed onto the entrance slit of a Czerny–Turner spectrometer, operated alternatively with a 150-groove mm^{-1} grating blazed at 300 nm (for tungsten lamp) or a 1200-grooves mm^{-1} holographic grating (for resonance absorption with iodine EDL, see below). The spectra were recorded by a CCD camera (Roper Scientific) with a 1024×1024 silicon detector chip (SiTE). The CCD can be operated either *statically*, recording individual spectra at pre-set times, or *time-resolved*, recording sequences of spectra at set intervals. The minimum time between consecutive spectra in time-resolved mode is 20 μs. The photolysis flash system contains two xenon flash tubes with a maximum output of 160 J per flash each. The energy of the flash can be varied by placing optical filters between the tube and the vessel, or by varying the charging voltage of the flash system. In these experiments, the typical flash energy was approximately 80 J.

Iodine atoms were produced in the reaction vessel by photolysis of mixtures of N_2 and I_2 at approximately 17 mbar. The number of iodine atoms produced by each photolysis flash was determined by time-resolved measurement of the loss of I_2 by absorption spectroscopy. For these measurements, the I_2 absorption spectrum between 350 and 650 nm was observed using the 150-groove mm^{-1} grating and the tungsten lamp. The spectral resolution in this configuration was approximately 0.8 nm, measured as the full width

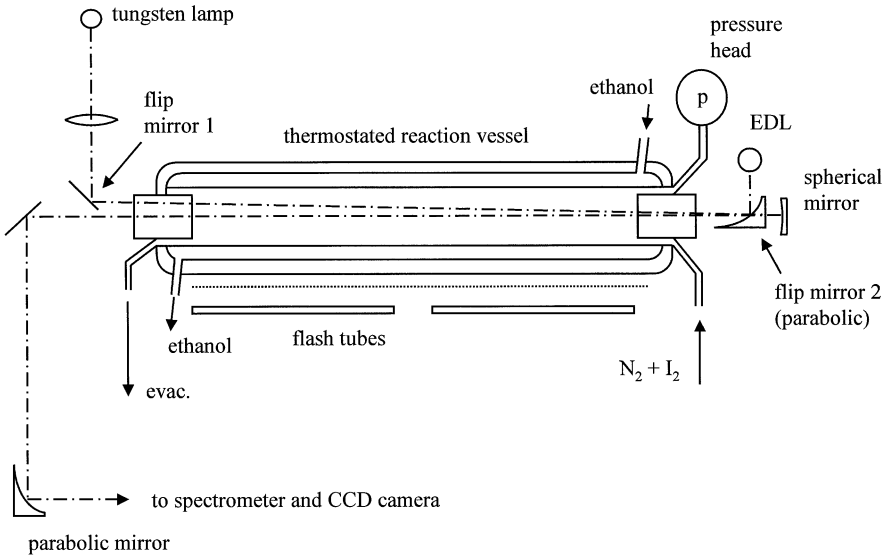

Fig. 1. Schematic diagram of the apparatus of the combined flash photolysis and resonance absorption set-up.

at half-maximum value (FWHM). Since a large section of the I_2 spectrum was recorded in these measurements (in contrast to the monochromatic measurements usually recorded by photomultiplier systems), baseline effects of the lamp could be minimized. Furthermore, a good signal-to-noise ratio for the time-resolved signal was achieved by numerical integration over parts of the observed I_2 absorption spectrum.

An RF-powered EDL and generator as described in [8] were used instead of the tungsten lamp for the resonance absorption set-up (flip mirror 2 in place and mirror 1 flipped aside, see Fig. 1). The atomic emission line of iodine at 183.038 nm has been the main focus of this study. Further emission lines are at 178.276, 179.909, 184.445, 187.641 and 206.163 nm. The last three of these were also readily observed, while the lines at 178.276 and 179.909 nm could only be observed with difficulty. The light of the EDL was passed through the reaction vessel once and then focussed into the spectrometer. It was analyzed using the 1200-grooves mm^{-1} holographic grating. With this grating, the dispersion of the spectrometer was sufficient so that the lines under study were well separated, even with the entrance slit opened up to 0.5 mm. Thereby, throughput of the spectrometer was optimized to compensate for loss of light of the optical system due to absorption, especially in the far-UV and vacuum UV (VUV). The line shape itself was not resolved in this setting and only spectrally integrated intensities could be measured:

$$I = \int_{\text{line}} \Phi(\nu)\ \mathrm{d}\nu \tag{1}$$

where $\Phi(\nu)$ is normalized to the integral line intensity I and describes the distribution of intensity over the line profile as a function of frequency ν. With the given grating (1200 grooves mm^{-1}) and the entrance slit set to 0.5 mm, the signal of the individual lines as recorded by the CCD chip was dominated by the instrument's spectral response function, with a FWHM of approximately 21.5 pixels ($\approx$ 0.5 mm on chip). The signals recorded by individual pixels were binned in hardware (on chip) and software (post processing) in order to improve the signal/noise ratio. Fig. 2 shows three typical recordings of intensity vs. time recorded at 183.038 nm at 0.5 ms per data point. The three traces were measured at three different concentrations of $[I_2]$. The con-

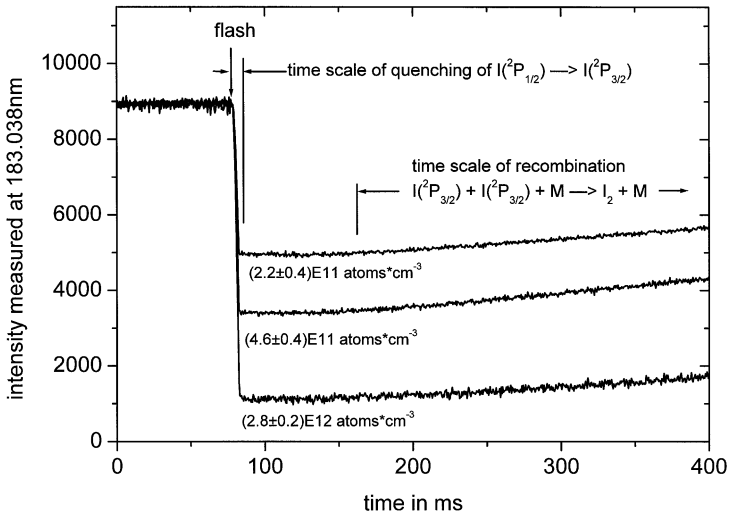

Fig. 2. Three time-resolved intensity measurements at 183.038 nm are shown. They were recorded at three different concentrations of [I_2] with correspondingly different concentrations of [I] under otherwise constant conditions. The time scale of the fast quenching of $I(^2P_{1/2}) + M \rightarrow I(^2P_{3/2}) + M$ and that of the recombination of $I(^2P_{3/2}) + I(^2P_{3/2}) \rightarrow I_2 + M$ are indicated. The intensity I which was used to calculate both relative absorption and *effective* absorbance was calculated as an average over a suitable time interval in between. Similarly, the reference intensity I_0 was determined using the time interval before the flash.

centrations of [I] as released by photolysis differ correspondingly. To record far-UV and VUV signals below 240 nm, the entire optical system was enclosed and purged with N_2 to suppress absorption by O_2. Absorption signals at 183.038 nm, as well as at 206.163 nm, during photolysis were recorded in time-resolved mode (Fig. 2). The intensity observed *before* (no iodine atoms $\Rightarrow$ measured intensity I_0) and *after* the flash (iodine atoms from photolysis $\Rightarrow$ measured intensity I) provided the data for calculating absorbance $A = \ln(I_0/I)$ or relative absorption $Q = (I_0 - I)/I_0$ $[= 1 - \exp(-A)]$. The experiments were performed in flow mode. A stable flow of I_2 in N_2 was produced by passing a flow of N_2 through a thermostated glass vessel ($T = 273.15$ K) containing I_2. This flow could be diluted by an additional flow of pure N_2. Flows were controlled using calibrated mass-flow controllers (MKS Instruments). Pressure in the vessels was measured with calibrated capacitance manometers (MKS Instruments). The I_2, resublimed p.a., was obtained from ACROS Organics, CAS No 7553-56-2. The N_2 was obtained from Messer-Griesheim (grade 4.8).

The design of the EDL has a side arm of 6 cm in length, which is well separated from the discharge region (Fig. 3). This side arm can be temperature-stabilized at different temperatures (see [7,8] for more details), enabling the vapor pressure of iodine in the lamp and discharge volume to be precisely controlled. This enables the dependence of self-absorption and self-reversal on partial pressure of iodine in the discharge volume to be studied.

3. Methods and results

3.1. Optimal operating conditions: minimizing self-absorption

The phenomena of self-absorption and self-reversal in atomic line sources result from the simultaneous presence of emitting atoms and lower-state atoms capable of absorption within the discharge volume of the lamp. Lower-state atoms, which are outside the plasma but still within the lamp volume, have a lower temperature than the emitting atoms within the plasma.

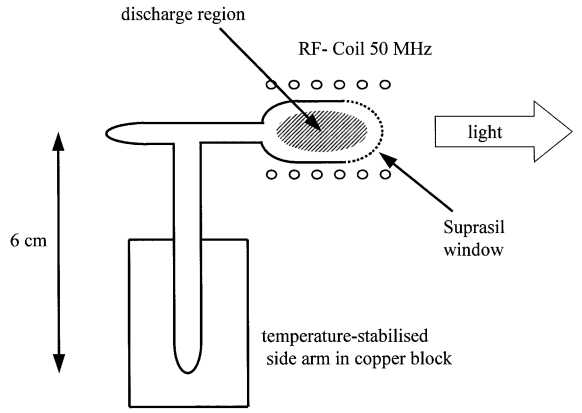

Fig. 3. The EDL consists of a discharge volume of approximately 18 mm in outer diameter and 35 mm in length. The discharge volume is connected to a side arm of approximately 6 cm in length, which is located in a thermostated block of copper. By thermostating the side arm of the lamp volume, the vapor pressure of iodine inside the lamp can be controlled.

Therefore, their absorption line profile is narrower than the emission line profile from the plasma and a self-absorbed, or even self-reversed line, results. The spatial distribution and relative concentrations of emitting and absorbing atoms critically depend on the partial pressure of the element (here iodine) within the discharge volume: The higher the partial pressure of the element is, the more lower-state atoms exist outside the emitting plasma. A more self-absorbed, or even self-reversed line, is the result. Revalde and Skudra [7] examined mercury line shapes as emitted by mercury EDL using a Fabry–Perot interferometer, a comparable type of RF generator, and the same lamp construction that is used for the iodine lamps in this study. They showed that within certain limits, self-absorption can be reduced by the use of higher-power RF fields, whereby lower-state atoms are transferred into higher-level states. A more efficient method of controlling self-absorption and self-reversal is provided by regulating the partial pressure of iodine in the lamp via the side-arm temperature [7,8]. The studies of Revalde and Skudra [7] demonstrated that self-*reversal* becomes less critical at partial pressures below 10^{-2} mbar, i.e. for I_2 at approximately 263 K. Therefore, in our studies the side-arm temperature was varied between ca. 243 and 268 K, corresponding to iodine vapor pressures of the order of 10^{-3}–10^{-2} mbar.

In our study, only the integrated signal of the iodine emission line was measured, as defined by Eq. (1). Therefore, an indirect method for estimating self-absorption and self-reversal was used. The relationship of Beer–Lambert applies to the absorption of *monochromatic* radiation, i.e.:

$$A(\nu) = \ln\left(\frac{I_0(\nu)}{I(\nu)}\right) = \sigma(\nu)\cdot N\cdot L \qquad (2)$$

where $\sigma(\nu)$ is the absorption cross-section of the absorber at frequency ν, N is the absorber concentration (molecules per volume) and L is the optical path length within the absorbing gas. $I(\nu)$ and $I_0(\nu)$ are the intensities at frequency ν measured with absorber and without absorber in the vessel, respectively. $A(\nu)$ denotes the Beer–Lambert absorbance at frequency ν. The relationship of Beer–Lambert does not apply to the case of *integrated* signals I and I_0 according to Eq. (1). However, under certain conditions a proportional relationship between absorber concentration N and an *effective* absorbance A_{eff}, formally calculated according to:

$$A_{\mathrm{eff}} = \ln\left(\frac{I_0}{I}\right) \propto N \qquad (3)$$

can be used and has to be empirically calibrated (calibration curve). Here I_0 and I are the integral intensities measured according to Eq. (1). Furthermore, if self-absorption occurs in the lamp, the situation is further complicated. The calibration curve relating the effective absorbance A_{eff} to the absorber concentration N then deviates from straight proportionality, displaying an increasingly reduced signal at higher absorber concentrations. In this case, it can be shown [9] that deviation from proportionality gets increasingly stronger with increasing self-absorption of the emission line under otherwise constant conditions.

Consequently, for decreasing side-arm temperatures, and therefore decreasing self-absorption under otherwise constant conditions, the effective absorbance calculated according to Eq. (3) should

approach the optimal estimate for a self-absorption-free measurement. Therefore, the concept for assessing self-reversal was:

1. Photolysis of I_2 in N_2 to produce constant amounts of $I(^2P_{3/2})$ and $I(^2P_{1/2})$ in the reaction vessel.
2. Measurement of the resulting effective absorbance $A_{\text{eff}} = \ln(I_0/I)$ as a function of side-arm temperature, i.e. by varying the extent of self-absorption and self-reversal.

In this chemical system, the photolysis of I_2 produces iodine atoms in ground ($^2P_{3/2}$) and metastable ($^2P_{1/2}$) states:

$$I_2 + h\nu \rightarrow \alpha \cdot I\left(^2P_{3/2}\right) + \beta \cdot I\left(^2P_{1/2}\right)$$

with $\alpha + \beta = 2$ and $h\nu$ designating the photolysing photon. The branching ratio defined by α and β depends on the spectrum of the photolysis flash, as well as on the internal energy of the I_2 molecule [10]. It can be shown (see below) that knowledge of α and β is not necessary for our studies. In our experiments, the excited metastable iodine atoms $I(^2P_{1/2})$ observed at 206.163 nm were most rapidly quenched by collisions (compare also [8]). The time scale of this collisional quenching depended on the mixture and was of the order of a few up to 100 μs. On the other hand, the recombination reaction

$$I\left(^2P_{3/2}\right) + I\left(^2P_{1/2}\right) + M \rightarrow I_2 + M$$

with a rate coefficient k of the order of 10^{-32}–10^{-29} $cm^3\ s^{-1}\ atom^{-1}$ [11] is slow and takes place on a time scale of several 100 ms. Fig. 2 illustrates the different time scales of these two effects. The quenching of iodine ($^2P_{1/2}$) was already completed on the intermediate time scale of our experiments, while the recombination reaction has not yet changed the concentration of iodine ($^2P_{3/2}$) significantly. Hence, both effects were negligible. I_0 was determined by averaging the values measured before the flash, while I was calculated as an average over a suitable time interval after the flash and before recombination started to be significant.

For each temperature setting, the effective absorbance at 183.038 nm following the photolysis of I_2 and the formation of $I(^2P_{3/2})$ was measured in time-resolved mode and averaged over at least 20 consecutive flashes under otherwise identical conditions. The concentration of $I(^2P_{3/2})$ produced by the flash was determined from knowledge of the photolysis rate of I_2. This had previously been measured using the absorption of I_2 between 350 and 650 nm. The I_2 concentration was stabilized to within $\pm 3\%$ and the flash energy was held constant during these experiments. The yield of $I(^2P_{3/2})$ per flash from I_2 could therefore be assumed to be constant within these error limits.

Fig. 4a,b displays six plots of effective absorbance vs. side-arm temperature as measured at six different absorber concentrations. The six traces are shown three at a time, and in the case of Fig. 4b, the lower two curves are translated vertically by $+0.25$ and $+0.45$, respectively, for clarity. The data clearly displays the behavior expected. The effective absorbance approaches a limiting maximum value at the lowest side-arm temperatures, indicating that the optimum operating conditions with minimum self-absorption have been reached. A further decrease in side-arm temperature only decreases the iodine concentration and the emission intensity of the discharge. The minimum temperature that could be reached with the present set-up was approximately 243 K. At side-arm temperatures between 246 and 248 K, the effective absorbance deduced clearly levels out, indicating that the optimum is reached. These temperatures correspond to an iodine vapor pressure of approximately 2.5×10^{-3} mbar. Under these conditions, self-absorption is minimal, whilst emission intensity is not yet significantly reduced. The same behavior was observed for all six individual data sets recorded at six different atomic iodine concentrations in the reaction vessel (ranging from 0.98×10^{11} to 2.8×10^{12} atoms cm^{-3}). Accordingly, it is assumed that self-absorption in the light source in the following analysis can be neglected.

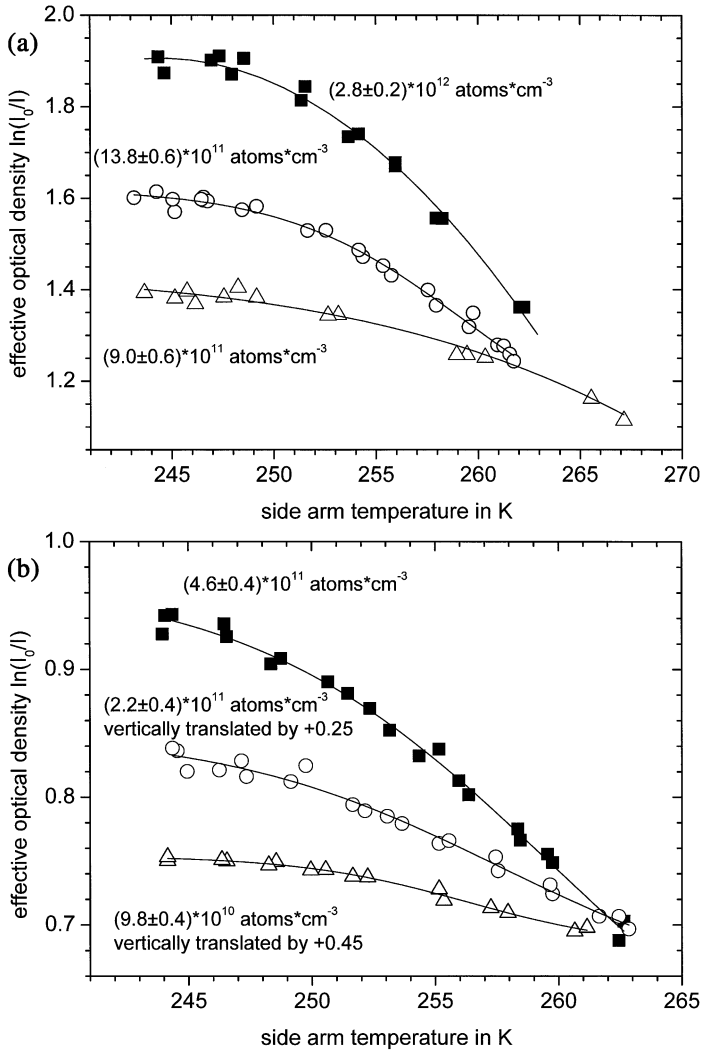

Fig. 4. (a, b) The effective absorbance $A_{\text{eff}} = \ln(I_0/I)$ for six different absorber concentrations (iodine atoms [I]) determined as a function of side-arm temperature under otherwise constant conditions. For clarity, the six traces are shown three at a time. In (b), the lower two curves are translated vertically by $+0.25$ and $+0.45$, respectively, for clarity.

3.2. Determination of emission temperature in the EDL

From each of the six data sets mentioned above, only the intensities measured under minimal self-absorption conditions (the 'low-temperature limits') were used for further analysis, and in the next step, line profiles of emission and absorption were taken into account.

At room temperature (≈ 300 K), the gas mixture in the lamp has a pressure of approximately 3 mbar, which corresponds to a concentration of ca. 7.25×10^{16} molecules cm^{-3}. The temperature of the plasma is most likely between 700 and 1400 K when the lamp is in operation. Under such conditions, the Lorentz line width is 0.0006 (at 700 K)–0.0009 cm^{-1} (at 1400 K), due to pressure broadening in the lamp, whereas the Doppler line width under the same conditions is more than two orders of magnitude larger (approx. 0.09–0.13 cm^{-1} at 700–1400 K).

The pressure in the reaction vessel was main-

tained at approximately 17 mbar, corresponding to a concentration of 4.11×10^{17} molecules cm^{-3}, which is approximately six-fold greater than the concentration in the lamp. The temperature was maintained at room temperature of 293 K. Even though the temperature in the vessel was significantly lower than the temperature in the lamp, the higher concentration led to a larger Lorentz line width of 0.0024 cm^{-1} (293 K) in the vessel. Yet again, as in the lamp, the corresponding Doppler line width was more than one order of magnitude greater (0.06 cm^{-1} at 293 K). Therefore, both the emission and absorption line profiles were clearly Doppler-dominated.

However, the Doppler width of the emission line in the EDL was greater than that of the absorption line by a factor of approximately 1.5–2. Therefore, it is expected that the absorbance values calculated according to $A_{\text{eff}} = \ln(I_0/I)$ and plotted vs. iodine concentration N in the reaction vessel do not follow the proportional relationship postulated in Eq. (3), despite the fact that self-absorption is already minimized and assumed to be negligible.

The data plotted in Fig. 5 clearly display this expected behavior. The effective absorbance deduced shows increasingly reduced values for higher concentrations and clearly deviates from proportional behavior. The values are not proportional to the absorber concentration N in the vessel. In view of finally deducing the oscillator strength and in order to understand and analyze this behavior quantitatively, the concept of relative absorption $Q = (I_0 - I)/I_0$, rather than absorbance $A = \ln(I_0/I)$, will be used in the following. These quantities are related according to $Q = 1 - \exp(-A)$. Relative absorption Q can be expressed in terms of Doppler profiles of emission and absorption lines {see [12] for a detailed derivation of Eqs. (4), (5a), (5b) and (6)}:

$$Q = \frac{I_0 - I}{I_0} = \frac{\int_{\text{line}} \Phi_0(\nu)\ \mathrm{d}\nu - \int_{\text{line}} \Phi_0(\nu) \cdot \exp(-k(\nu) \cdot L)\ \mathrm{d}\nu}{\int_{\text{line}} \Phi_0(\nu)\ \mathrm{d}\nu} \tag{4}$$

where

$$\Phi_0(\nu) = \Phi_0 \cdot \exp\left(-4 \cdot \ln 2 \cdot \left(\frac{\nu - \nu_0}{\delta\nu_{\text{D,em}}} \right)^2 \right) \tag{5a}$$

represents the emission Doppler profile of maximum intensity Φ_0, of width $\delta\nu_{\text{D,em}}$ and centered at ν_0,

$$k(\nu) = k_0 \cdot \exp\left(-4 \cdot \ln 2 \cdot \left(\frac{\nu - \nu_0}{\delta\nu_{\text{D,abs}}} \right)^2 \right) \tag{5b}$$

represents the absorption Doppler profile of maximum absorption k_0 at the line center ν_0 and of width $\delta\nu_{\text{D,abs}}$, and where L in Eq. (4) is the optical path length in the absorbing medium.

The variable α is introduced [see Eqs. (6) and (8)] to express the dependence of Q on emission and absorber temperature. It is defined as the ratio of the Doppler width in emission to that in absorption, and can be expressed in terms of the two absolute temperatures:

$$\alpha = \frac{\delta\nu_{\text{D,em}}}{\delta\nu_{\text{D,abs}}} = \sqrt{\frac{T_{\text{em}}}{T_{\text{abs}}}} \tag{6}$$

This notation is used in listing the 'low-temperature limits' from the six data sets expressed in terms of relative absorption $Q(\alpha)$ in Table 1, along with the corresponding absorber concentration N.

The instrument response function, and the fact that the line profiles are not spectrally resolved, are taken into account in Eq. (4) by integrating over the line profiles according to Eq. (1). Note that the intensity I measured with absorbing atoms in the vessel is expressed in terms of the incident emission-line profile. This is multiplied by a Beer–Lambert factor, which is modulated by

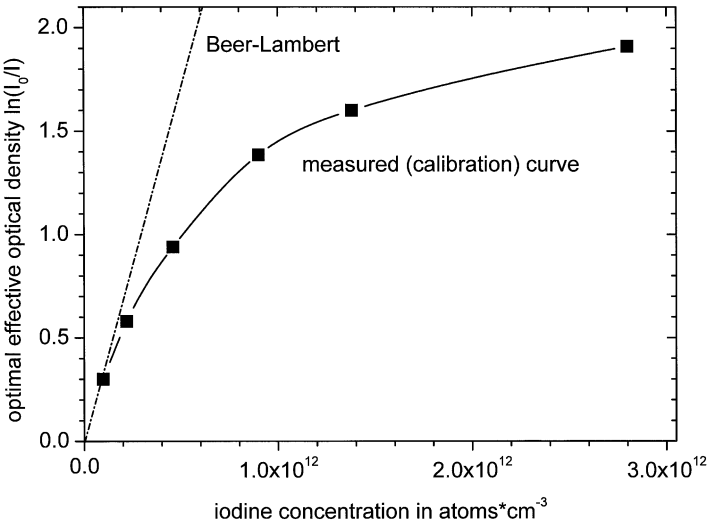

Fig. 5. The *optimal* effective absorbance $A_{\text{eff}} = \ln(I_0/I)$ for $T < 245$ K plotted as a function of absorber concentration in the reaction vessel. The straight line represents a Beer–Lambert, or at least a proportional, relationship between absorbance and absorber concentration. The data measured display increasingly reduced values for large absorber concentrations, deviating from a proportional behavior.

the profile of the absorbing line $k(\nu)$. The absorber line profile according to Eq. (5b) contains the maximum value k_0, which is proportional to the absorber concentration N in the vessel:

$$k_0 \propto N \tag{7}$$

After inserting Eqs. (5a) and (5b) into Eq. (4), a relationship between the experimentally measured integrated intensities I and I_0 and [via k_0 and Eq. (7)], the absorber concentration N is defined. Using a series expansion, Eq. (4) can be transformed into [12]:

$$Q(\alpha) = \frac{I_0 - I}{I_0} = \sum_{n=1}^{\infty} \frac{(-1)^{n+1} \cdot (k_0 \cdot L)^n}{n! \cdot \sqrt{1 + n \cdot \alpha^2}} \tag{8}$$

If α is known, this expression can then be solved for k_0 using $Q(\alpha)$ and L values determined from the experiment. Yet by reversing the argument, Eq. (8) can also be numerically solved for k_0, using:

1. The data measured for $Q(\alpha) = (I_0 - I)/I_0$ and L for the different concentrations in the reaction vessel; and
2. A value for α dependent on an assumed (trial) emission temperature (the absorber temperature being known).

Then the proportionality postulated by Eq. (7) can be checked. If the resulting values for k_0 are not proportional to the known absorber concentration, then the value assumed for the emission temperature is not correct. On the contrary, the better the proportionality between k_0 and N, the better the estimation of the emission temperature.

Table 1
Relative absorption Q(α) at 183.038 nm as a function of absorber concentration N

Absorber concentration N [10^{11} atoms cm^{-3}]	Relative absorption $Q(\alpha)$ [dimensionless]
0.98 ± 0.1	0.2607 ± 0.0002
2.2 ± 0.4	0.4423 ± 0.0004
4.6 ± 0.4	0.6082 ± 0.0005
9.0 ± 0.6	0.7517 ± 0.0004
13.8 ± 0.6	0.8002 ± 0.0004
28.0 ± 1.0	0.8498 ± 0.0005

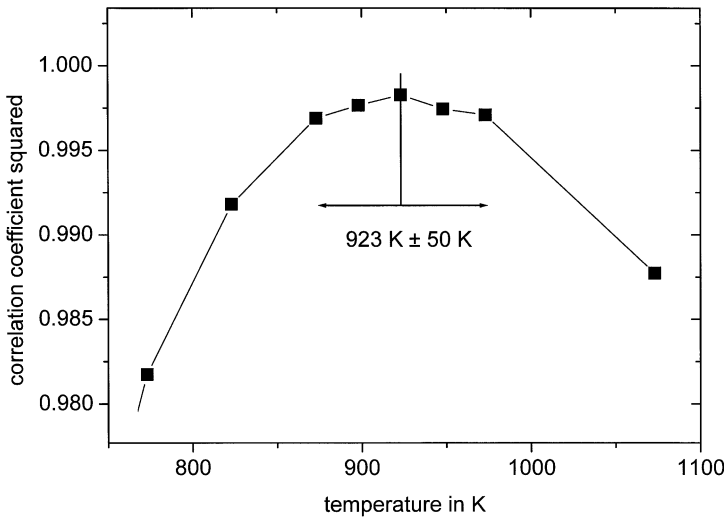

Fig. 6. The square of the correlation coefficient achieved for a linear fit $k_0 = \sigma \cdot N$ (with σ as proportionality constant) plotted against assumed emission temperature. At $T = 923$ K, it clearly reaches a maximum, indicating that the proportionality is best, and therefore the best estimate for the emission temperature is reached. The accuracy is conservatively estimated to be ± 50 K, yielding $T_{em} = 923 \pm 50$ K.

This analysis was performed for various values of the emission temperature. The degree of proportionality was estimated by performing a linear fit according to $k_0 = \sigma \cdot N$ (with σ as proportionality constant) and by taking the square of the correlation coefficient that resulted from the fit as a measure for proportionality. For $T_{em} = 923 \pm 50$ K, the best correlation was achieved with a maximum correlation coefficient squared of 0.9983. Within the error limits of ± 50 K, the

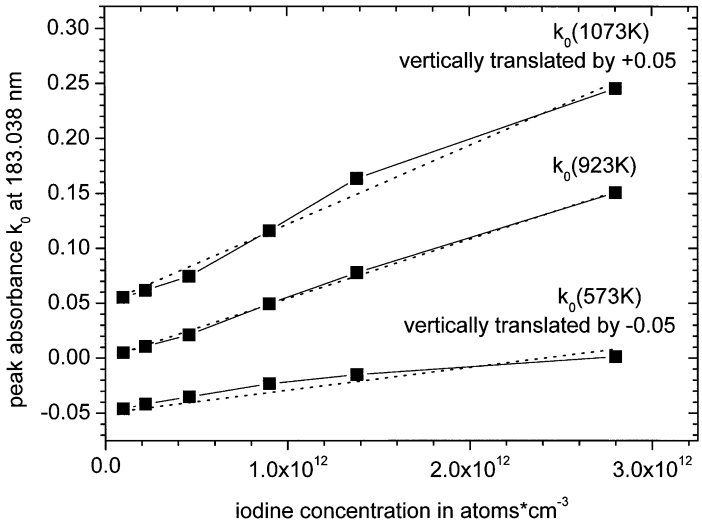

Fig. 7. Maximum of the absorption profile, k_0, as determined from the measured integral intensities plotted vs. absorber concentration in the reaction vessel. Depending on the source temperature chosen in the determination of k_0, the data for k_0 display a different curvature. The best estimate for the source temperature is determined by minimizing the deviation from proportionality. In addition to the best-fit result, two other cases at different temperatures are shown to illustrate the method. The latter are vertically translated by $+0.05$ and -0.05, respectively, for clarity.

square of the correlation coefficient significantly decreased to 0.997 (see Fig. 6). In Fig. 7, k_0 is plotted vs. concentration for this optimal estimate, as well as for two different values that are assumed for emission temperature in order to further illustrate the method.

3.3. Determination of oscillator strength

The oscillator strength f, the maximum absorption k_0 and the concentration N are related by the following expression [13–15]:

$$f = \frac{m \cdot c}{2\sqrt{\pi \cdot \ln 2} \cdot e^2} \cdot \delta\nu_{\mathrm{D,abs}} \cdot \frac{k_0}{N}$$

in cgs (Gauss) units

$$= \frac{m \cdot c \cdot 4\pi\varepsilon_0}{2\sqrt{\pi \cdot \ln 2} \cdot e^2} \cdot \delta\nu_{\mathrm{D,abs}} \cdot \frac{k_0}{N}$$

in SI units

$$\approx 40.11 \frac{s}{cm^2} \cdot \delta\nu_{\mathrm{D,abs}} \cdot \frac{k_0}{N} \qquad (9)$$

where m is the electron mass, c the velocity of light in vacuum and ε_0 the permittivity of the vacuum. Introducing the proportionality coefficient σ yields:

$$f \approx 40.11 \frac{s}{cm^2} \cdot \delta\nu_{\mathrm{D,abs}} \cdot \sigma \qquad (10)$$

σ resulted from the best linear fit (corresponding to the best-estimated source temperature) and relates k_0 and N [see Eq. (7)]. The proportionality coefficient then becomes:

$$\sigma = (5.42 \pm 0.8) \times 10^{-14} \quad \mathrm{cm^2\ atom^{-1}}$$

where the error limits correspond to the error limits estimated for the emission temperature. Therefore:

$$f = (3.87 \pm 0.57) \times 10^{-3}$$

As inferred from the definition of the proportionality coefficient σ, and as already anticipated by the use of the Greek letter σ, the proportionality coefficient represents the Beer–Lambert absorption cross-section of atomic iodine at the peak of the absorption profile.

4. Discussion

Revalde and Skudra [7] examined a mercury EDL with a generator and lamp similar to those used in the present study. They used a Fabry–Perot interferometer to examine the spectral shape of the emission lines. They reported that at mercury partial pressures below 10^{-2} mbar, no self-reversal was detectable. In their study, the degree of self-reversal was determined by direct measurement of a dip at the center of the line. Absence of a dip at the line center indicated absence of self-reversal. However, the effect of moderate self-absorption (long before self-reversal in the form of a dip at the line center occurs) cannot be measured by this technique.

In comparison to this, our method using the effect of self-reversal and self-absorption on measured effective absorbance $A_{\mathrm{eff}} = \ln(I_0/I)$ [Eq. (3)] is more sensitive. This is because even a slightly self-absorbed line (still not self-reversed and still without the development of a dip at the line center) is already deformed in such a way that the intensity in the vicinity of the line center is reduced in comparison to the intensity of the flanks. The absorption of a narrower (colder) absorber line leads to a weaker absorption signal, because the intensity of the non-absorbed flanks of the emission line dominates the integrated signal. Following this argument, the method of examining the effect on deduced effective absorbance A_{eff} can be used to assess self-*reversal*, as well as the much smaller effect of self-*absorption*. It is a more sensitive method than the direct measurement of self-reversal via the detection of a dip at the line center.

For this reason, the critical partial pressure reported by Revalde and Skudra [7] for non-self-reversed conditions is considered only an upper limit for conditions, which are free of self-absorption. Hence, the reported value of 10^{-2} mbar in [7], determined under non-self-*reversed* conditions

for mercury emission, and our value of 2.5×10^{-3} mbar for self-*absorption*-free (or at least minimized self-absorption) conditions for iodine emission are in rather good agreement.

In the present study, we determined the discharge temperature to be $T_{em} = (923 \pm 50)$ K. Clyne and Townsend [16] report an estimated emission temperature for microwave discharges of approximately 600 K, but this strongly depended on the actual discharge conditions. Due to this major uncertainty, they avoided the use of discharge source temperature by using fluorescence light from a temperature-stabilized fluorescence source instead of light emitted directly from a discharge. Skudra (personal communication, 2001) reports that with the type of EDL used in his study, as well as in ours, emission temperatures of 800–1400 K are expected, depending on the generator current and lamp geometry. In the study of Revalde and Skudra [7], a strongly self-reversed line profile of mercury at 253.7 nm is shown. Estimating a line width (FWHM) in spite of self-reversal by approximately extrapolating the self-reversed line to a more or less non-self-absorbed profile, yields a FWHM value of ca. 0.06–0.07 cm^{-1}, which corresponds to a source temperature of 900–1200 K. These temperature estimates are in good agreement, considering that the generators and lamps are handmade, and therefore are not strictly comparable.

To the best of our knowledge, there are only two previous publications reporting the oscillator strength for the 183.038 nm transition of iodine. Clyne and Townsend [16] reported a value of $(1.67 \pm 0.23) \times 10^{-3}$, whereas Lawrence [17] reported a value that is one order of magnitude larger, $(1.21 \pm 0.5) \times 10^{-2}$. The method applied by Clyne and Townsend is similar to ours. They used the proportionality between a known absorber concentration and the maximum absorption measured k_0. Using fluorescence rather than a discharge line source, they avoided the problem of unknown source temperature, and at the same time reduced self-absorption and self-reversal. They used relative intensities of multiplet transitions in the resonance fluorescence light as a diagnostic for the absence of self-reversal. Thus, with both above-mentioned methods, the measurements define optimum conditions under which an effect of self-absorption can no longer be detected, but cannot be completely excluded either.

However, in the analysis, one significant difference between the two methods remains. If in our measurements a slight self-absorption in the EDL remained that was neglected in the analysis, this would show up as a remaining non-proportional behavior of the deduced k_0 with respect to concentration. As a consequence of the proportionality fitting procedure that we used for the determination of the source temperature, this would lead to an overestimation of emission temperature. Non-proportionality caused by self-absorption would be misinterpreted as being caused by a higher source temperature. In that case, a slightly broader Doppler profile (determined by the overestimated source temperature) would be used in Eq. (2) instead of the true self-absorbed emission profile. As a result, the values for k_0, σ, and therefore f, would also be overestimated. In this view, our result should be considered as an upper limit for the oscillator strength.

On the other hand, Clyne and Townsend's [16] data still display a non-proportionality at higher concentrations. Due to their approach, the emission temperature, as well as the absorber temperature, was known. Therefore, uncertainties in source temperature cannot be responsible for this deviation. Rather, this behavior might be indicative of a remaining and unaccounted for self-absorption. This would then imply that the inferred oscillator strength was determined for sub-optimal conditions, and therefore f would be underestimated. This interpretation is further supported by the discussion in [16], where it is stated that the iodine emission lines used in the work (178.276 and 183.038 nm) were generated by photolysis of ICl with 121.6 nm radiation, which can give excited iodine atoms with a significant excess of kinetic energy. These lines, therefore, might be much broader than 300 K Doppler lines, which were assumed in their analysis. This would clearly lead to an underestimation of f values. Following these arguments, the discrepancy between Clyne and Townsend's result [16] and ours can be

resolved when considering them as upper and lower limits, respectively. At the same time, the reliability and accuracy of both approaches and methods appears to be very comparable. We come to the conclusion that their result and ours complement each other, and thereby determine the oscillator strength f more accurately to be:

$(1.67 \pm 0.23) \times 10^{-3}$ [16]

$$< f < \times (3.87 \pm 0.57) \times 10^{-3} \quad \text{(this work)}$$

Consequently, our result for the maximum absorption cross-section has to be interpreted as an upper limit of $\sigma < (5.42 \pm 0.8) \times 10^{-14}$ cm^2 atom^{-1}.

The disagreement between the result of Lawrence [17] on the one hand, and those of Clyne and Townsend [16] and our work on the other hand, is not easily understood. When comparing the results of [17] and [16], it is surprising that their values for bromine lines agree very well, while those for iodine disagree by one order of magnitude. In [16], it was shown that this discrepancy could not be explained by broader Doppler profiles, as inferred from the generation method of iodine atoms.

5. Conclusions

The optimal operating conditions for an RF-powered electrodeless discharge lamp were determined, resulting in minimized self-absorption of emission lines. A method was developed to estimate the source temperature that governs the Doppler line width. The absorption coefficient at the center of the absorption line and the corresponding oscillator strength for the 183.038-nm resonance absorption transition were determined to be $\sigma < (5.42 \pm 0.8) \times 10^{-14}$ cm^2 atom^{-1} and $(1.67 \pm 0.23) \times 10^{-3}$ [16] $< f < (3.87 \pm 0.57) \times 10^{-3}$ (this work). These results will be used to further improve the examination of iodine ozone chemistry, including the determination of absorption cross-sections of different iodine oxides.

Acknowledgements

This work was partially funded by the German Space Agency DLR through its support of the SCIAMACHY project, the European Union, the German Ministry of Education and Science (Project LVA-97-006), and by the University and the State of Bremen. The authors wish to express their gratitude to Prof J. Bleck-Neuhaus for many fruitful and inspiring discussions.

References

[1] S.P. Sander, Kinetics and mechanism of the IO + IO reaction, J. Phys. Chem. 90 (1986) 2194–2199.
[2] B. Laszlo, M.J. Kurylo, R.E. Huie, Absorption cross-section, kinetics of formation, and self-reaction of the IO radical produced via the laser photolysis of $N_2O/I_2/N_2$ mixtures, J. Phys. Chem. 99 (1995) 11701–11707.
[3] S. Himmelmann, J. Orphal, H. Bovensmann, A. Richter, A. Ladstaetter-Weissenmayer, J.P. Burrows, First observation of the OIO molecule by time-resolved flash photolysis absorption spectroscopy, Chem. Phys. Lett. 251 (1996) 330–334.
[4] M.H. Harwood, J.B. Burkholder, M. Hunter, R.W. Fox, A.R. Ravishankara, Absorption cross-sections and self-reaction kinetics of the IO radical, J. Phys. Chem. A 101 (1997) 853–863.
[5] P. Spietz, S. Himmelmann, U. Gross, J. Orphal, J.P. Burrows, Study of iodine oxides and iodine chemistry using flash photolysis and time-resolved absorption spectroscopy (abstract), Ann. Geophys. 16 (Suppl. II) (1998) C722.
[6] R.A. Cox, W.J. Bloss, R.L. Jones, D.M. Rowley, OIO and the atmospheric cycle of iodine, Geophys. Res. Lett. 26 (13) (1999) 1857–1860.
[7] G. Revalde, A. Skudra, Optimization of mercury vapor for high-frequency electrodeless light sources, J. Phys. D: Appl. Phys. 31 (1998) 3343–3348.
[8] U. Gross, A. Ubelis, P. Spietz, J.P. Burrows, Iodine and mercury resonance lamps for kinetics experiments and their spectra in the far ultraviolet, J. Phys. D: Appl. Phys. 33 (2000) 1588–1591.
[9] P.W.J.M Boumans, Excitation of spectrain: E.L. Grove (Ed.), Analytical Emission Spectroscopy Part II, Marcel Dekker, New York, 1972. Chapter 6.
[10] T.F. Hunter, C.M. Leong, Absolute yields of $I(^2P_{1/2})$ in I_2 photodissociation using a laser optoacoustic technique, Chem. Phys. 111 (1987) 145–153.
[11] W.G. Mallard, F. Westley, J.T. Herron, R.F. Hampson, D.H. Frizzell, NIST standard reference database 17NIST Chemical Kinetics Database Version 2Q98, US Department of Commerce, Technology Administration, NIST Standard Reference Data, Gaithersburg, MD, 1998.

[12] A.C.G. Mitchell, M.W. Zemansky, Resonance Radiation and Excited Atoms, Cambridge University Press, 1972.
[13] J.D. Ingle Jr, S.R. Crouch, Spectrochimical Analysis, Prentice Hall International Editions, London, 1988. Appendix F, 563 pp.
[14] A. Thorne, U. Litzén, S. Johansson, Spectrophysics: Principles and Applications, Springer, Berlin, Heidelberg, New York, 1999, pp. 175–179.
[15] M. Pinta, Atomic Absorption Spectrometry, Adam Hilger, London, 1975, pp. 7–8.
[16] M.A.A. Clyne, L.W. Townsend, Determination of atomic oscillator strengths using resonance absorption with a Doppler line source: transitions of Br and I$(n + 1)s-np^5$, J. Chem. Soc. Faraday Trans. II 70 (1974) 1863–1881.
[17] G.M. Lawrence, Resonance transition probabilities in intermediate coupling for some neutral non-metals, Astrophys. J. 148 (1967) 261.